

## Study of neutron rich Cadmium isotopes and the possible $N=82$ shell quenching

---

**Tomás R. Rodríguez\***

*GSI Helmholtzzentrum für Schwerionenforschung, D-64259 Darmstadt, Germany*

*Departamento de Física Teórica, Universidad Autónoma de Madrid, E-28049 Madrid, Spain*

*E-mail: [t.rodriiguez@gsi.de](mailto:t.rodriiguez@gsi.de)*

**J. Luis Egido**

*Departamento de Física Teórica, Universidad Autónoma de Madrid, E-28049 Madrid, Spain*

**Andrea Jungclaus**

*Instituto de Estructura de la Materia-CSIC, E-28006 Madrid, Spain*

We study the chain of Cadmium isotopes from  $N = 50 - 82$  magic numbers with modern beyond mean-field methods with the Gogny D1S interaction. In a previous publication [1] we showed that experimental excitation energies and reduced transition probabilities of the first  $2^+$  states are qualitatively well described in the whole chain assuming axial symmetry. Moreover, the anomalous behavior of the  $2^+$  energies close to  $N = 82$  is well reproduced without assuming any shell quenching. Here we justify the axial approximation by analyzing the potential energy surfaces in the triaxial plane and summarize the main results obtained in [1].

*11th Symposium on Nuclei in the Cosmos, NIC XI*

*July 19-23, 2010*

*Heidelberg, Germany*

---

\*Speaker.

During the last decade different theoretical and experimental studies suggested the possible  $N = 82$  shell quenching in the neutron rich Cadmium isotopes. Hence, some r-process simulations gave a better agreement with solar abundance distribution for  $A=130$  peak if a reduction of  $N = 82$  shell closure was assumed [2, 3]. Also, mass formulae based on Skyrme interactions assuming spherical symmetry predicted a reduction of the spherical gap in this region [4, 5]. Finally, experimental high  $Q$ -values and anomalous behavior of the  $E(2^+)$  energies for neutron rich Cd isotopes could be hints for  $N = 82$  shell quenching [6, 7]. However, recent measurements of the  $E(2^+)$  for  $^{130}\text{Cd}$ , masses for  $^{132}\text{Sn}$  and  $^{134}\text{Sn}$  and spectroscopic factors of  $^{133}\text{Sn}$  restored  $N = 82$  as a good magic number [8, 9, 10]. Furthermore, the small values of the excitation energies for the Cd isotopes in this region has been recently interpreted as an onset of a slight prolate deformation of the  $^{130}\text{Cd}$  nucleus due to its singular single particle configuration [1]. These results were obtained with state-of-the-art beyond mean-field methods using the Gogny D1S interaction [11] and assuming axial symmetry. In this contribution we summarize the main results given in Ref. [1] and we also show the shape evolution of the Cd isotopes in the triaxial plane supporting the use of axial calculations in this case.

First we sketch briefly the method used for calculating the nuclear states, namely, generating coordinate method with particle number and angular momentum projected product-type wave functions (GCM-PNAMP) [12, 13, 14]. We start by building a set of Hartree-Fock-Bogoliubov (HFB) intrinsic wave functions  $\{|\Phi(\beta, \gamma)\rangle\}$  along the quadrupole deformation parameters  $(\beta, \gamma)$ . These HFB intrinsic states are found by solving the so-called constrained particle number variation after projection equations (PN-VAP)  $\delta(E^{N,Z}(|\Phi(\beta, \gamma)\rangle)) = 0$  [15]. Gogny D1S was used as the underlying interaction. This set of intrinsic states can be used to explore the energy landscape in the triaxial plane. In Figure 1 we show the PN-VAP energy as a function of deformation  $(\beta, \gamma)$  for  $N = 50 - 82$  Cd isotopes. We see that increasing the number of neutrons from  $N = 50$  magic number an axial prolate deformed minimum is developed and remains nearly constant at  $\beta \approx 0.18$  in a wide range of isotopes ( $N = 56 - 72$ ). Then, this minimum evolves towards a spherical configuration corresponding to the  $^{130}\text{Cd}$  semi-magic nucleus. Moreover, a slight softening of the potential energy surfaces is observed in the mid-shell isotopes although the main evolution occurs along the axial path. Therefore, we expect that the influence of triaxial effects in this isotopic chain will not be very relevant for the ground state bands. The next step is the computation of the excitation energies and transition probabilities of the first  $2^+$  states for the whole isotopic chain. This is done by mixing the axial states ( $\gamma = 0^\circ, 60^\circ$ ) which are also particle number and angular momentum projected, namely:

$$\sum_{\beta'} (\mathcal{H}^{I,N,Z}(\beta, \beta') - E^{I,N,Z}) \mathcal{N}(\beta, \beta') f^{I,N,Z}(\beta') = 0 \quad (1)$$

where  $\mathcal{H}^{I,N,Z}(\beta, \beta')$  and  $\mathcal{N}^{I,N,Z}(\beta, \beta')$  are the GCM energy and norm overlaps for given values of angular momentum  $I$ , number of proton ( $Z$ ) and neutrons ( $N$ ),  $E^{I,N,Z}$  are the computed energy spectra and the coefficients  $f^{I,N,Z}$  are used for calculating other observables - $B(E2)$  for example- within the GCM framework [12].

In Figure 2(a)-(b) we show the calculated and experimental -where available [16]- excitation energies and  $B(E2)$  for the Cd isotopes. We obtain a very good qualitative agreement between theoretical and experimental results along the whole isotopic chain. However, the calculations give

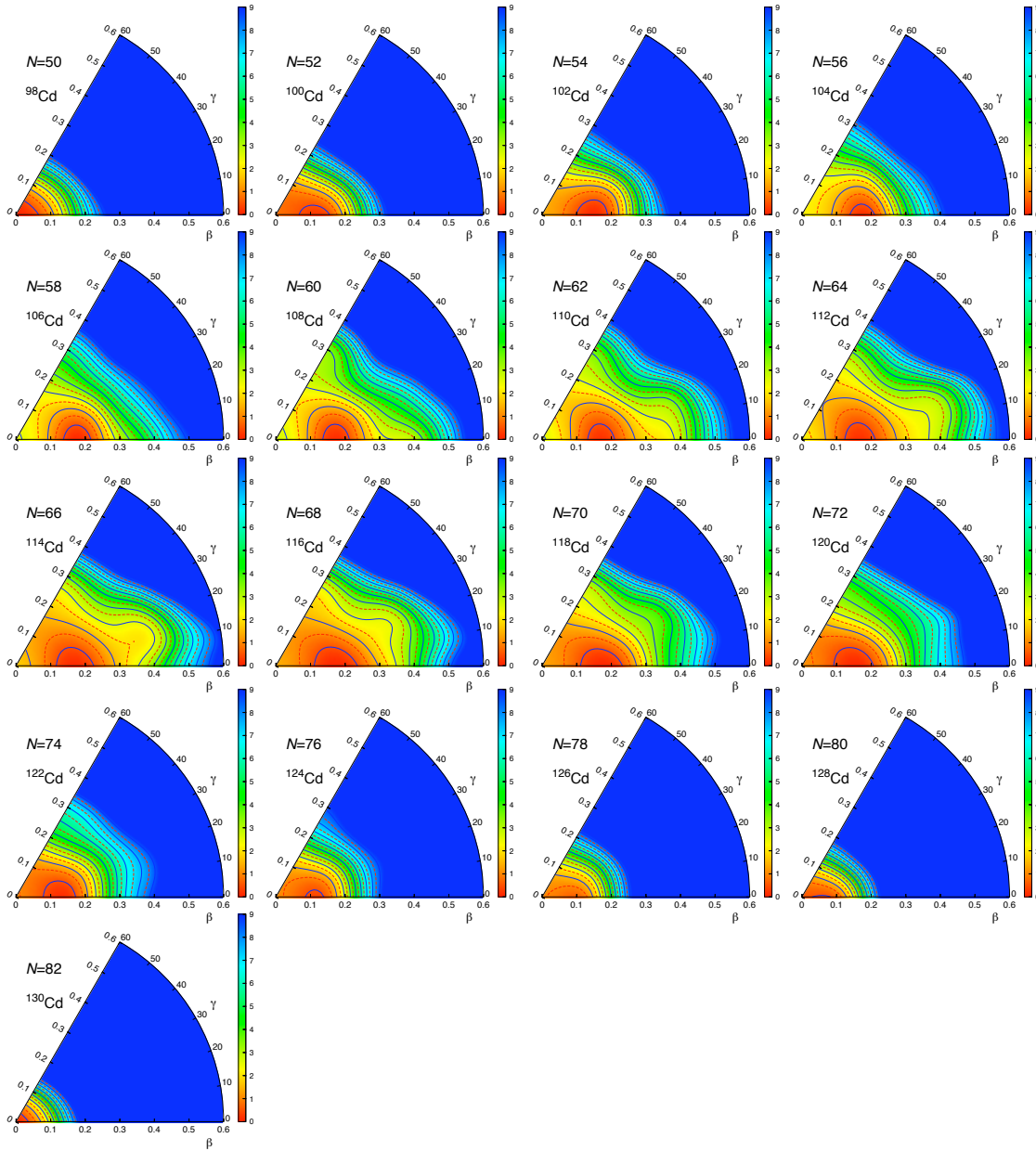


**Figure 1:** Potential Energy Surfaces in the  $(\beta, \gamma)$  plane for the Cd isotopic chain. Color scale is in MeV and contour lines are separated by 0.5 MeV. The energies are normalized to the minimum of each surface.

larger excitation energies due to the lack of time-reversal symmetry breaking and that the angular momentum projection is performed after the variation which provide smaller moments of inertia than the full self-consistent ones [17, 18]. In both experimental and theoretical results we observe the increase of collectivity from  $N = 50$  magic number with enlarging the number of neutrons, having smaller values for  $E(2^+)$  and correspondingly larger  $B(E2)$  values. We can distinguish a parabolic dependence from  $N = 50 - 58$  which corresponds to the filling of the  $g_{7/2}$  shell and a rather flat behavior between  $N = 60 - 70$  -filling  $d_{5/2}$ ,  $d_{3/2}$ ,  $s_{1/2}$  shells. More interestingly, the

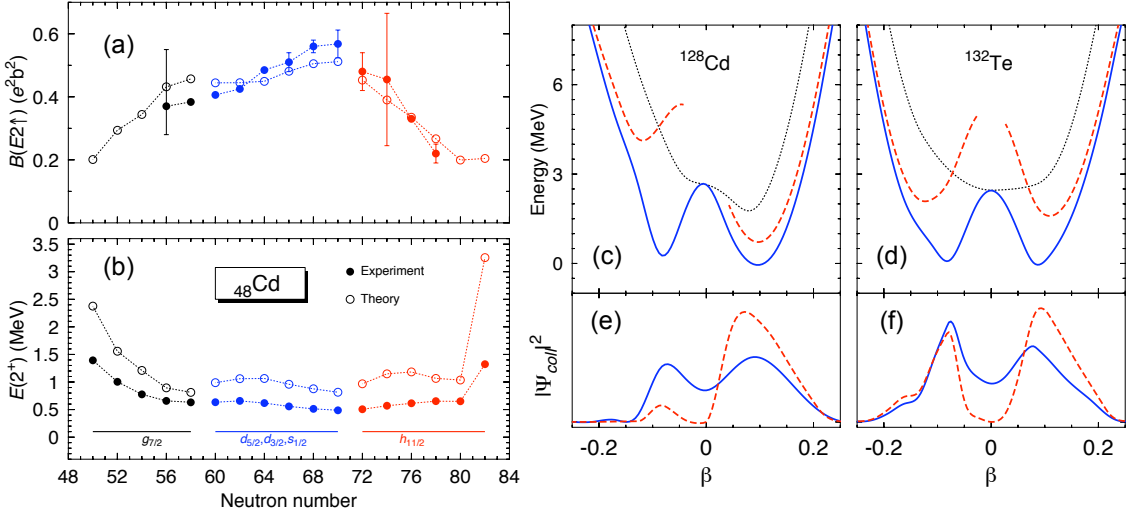


**Figure 2:** (a) Reduced transition probabilities  $B(E2)$  and (b) excitation energies of the first  $2^+$  state for  $^{98-130}\text{Cd}$  isotopes. Experimental values are taken from Ref. [16]. Potential Energy Surfaces -PN-VAP (dotted black),  $I = 0$  (full blue),  $I = 2$  (dashed red)- and collective wave functions as a function of axial quadrupole deformation  $\beta$  for (c)-(e)  $^{128}\text{Cd}$  and (d)-(f)  $^{132}\text{Te}$ . PES are normalized to the GCM-PNAMP ground state energies.

observed anomalous deviation from the parabolic trend between  $N = 72 - 82$  -filling  $h_{11/2}$  shell- and the decrease of the excitation energy for  $^{128}\text{Cd}$  are reproduced by the calculations. To shed light on this behavior we compare potential energy surfaces (PES) and collective wave functions of the ground and first  $2^+$  states for  $^{128}\text{Cd}$  and  $^{132}\text{Te}$  ( $N = 80$ ). The latter presents a normal behavior close to  $N = 82$  shell closure. In Fig. 2(c)-(d) we observe that  $J = 0$  PES have two almost degenerated minima with the same  $\beta$  deformation and different sign for both nuclei. We also see that this balance is kept for  $J = 2$  PES in  $^{132}\text{Te}$  but in  $^{128}\text{Cd}$  the prolate configuration is favored. Once the GCM is performed (Fig. 2(e)-(f)) we obtain spherical states in average for both ground states and also for  $2^+$  state in  $^{132}\text{Te}$ , but a slightly prolate deformed  $2^+$  state for  $^{128}\text{Cd}$ . This fact can explain the anomalous behavior of the  $E(2^+)$  in Cadmium isotopic chain.

Concerning the  $N = 82$  shell quenching, in Fig. 3 we show the single particle energies as a function of the axial quadrupole deformation calculated for  $^{128}\text{Cd}$  which are very similar to the ones for  $^{132}\text{Te}$  (not shown). Hence, we observe that the spherical shell gap remains as large as in  $^{132}\text{Te}$  case, where a normal behavior of the  $E(2^+)$  is found. In this figure we also see that due to the rising of the  $\nu p_{1/2}$  and  $\pi s_{1/2}$  orbits, we find beyond  $\beta \approx -0.15$  a double closed shell configuration for  $^{128}\text{Cd}$ . Therefore, oblate shapes are not energetically favored for  $I = 2$  as we showed in Fig. 2(c)-(e). This is not the case for the isotone  $^{132}\text{Te}$  where the proton Fermi level lies within the  $\pi g_{7/2}$  orbits and therefore, it is a balance between prolate and oblate configurations. Hence, the anomalous behavior of the  $E(2^+)$  observed while approaching the  $N = 82$  shell closure can be explained by the special onset of slight deformation in this specific nucleus and not to a shell quenching in this region.

In summary, we have presented state-of-the-art beyond mean field calculations from shell to shell  $N = 50 - 82$  for Cd isotopes with the Gogny D1S interaction. We have analyzed the potential

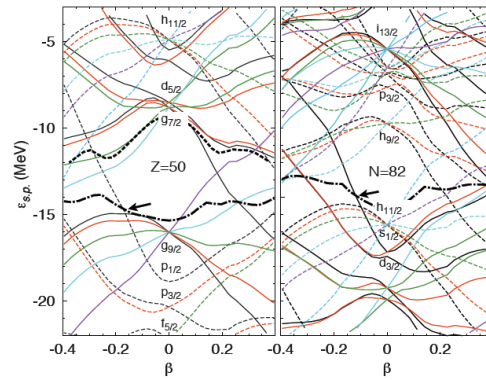


**Figure 3:** Single particle energies for (a) protons and neutrons (b) as a function of the deformation for  $^{128}\text{Cd}$ . The thick dotted dashed lines correspond to the Fermi level of the  $^{128}\text{Cd}$  while the dashed line corresponds to the proton Fermi level for  $^{132}\text{Te}$ .

role of the triaxiality in this isotopic chain. Finally, we propose the appearance of a slight prolate deformation in  $^{128}\text{Cd}$  to explain the anomalous behavior of the  $E(2^+)$  systematics without finding a spherical  $N = 82$  shell quenching in neutron rich Cadmium isotopes.

The authors acknowledge financial support from the Spanish Ministerio de Educación y Ciencia under contracts FPA2009-13377-C02-01, FPA2009-13377-C02-02, by the Spanish Consolider-Ingenio 2010 Programme CPAN (CSD2007-00042) and within the Programa de Ayudas para Estancias de Movilidad Posdoctoral 2008 (T.R.R).

## References

- [1] T. R. Rodríguez, J. L. Egido, A. Jungclaus, Phys. Lett. B 668, 410 (2008)
- [2] B. Chen et al., Phys. Lett. B 355, 37 (1995).
- [3] B. Pfeiffer, K.-L. Kratz and F.-K. Thielemann, Z. Phys. A 357, 235 (1997).
- [4] J. Dobaczewski, I. Hamamoto, W. Nazarewicz and J.A. Sheik, Phys. Rev. Lett. 72, 981 (1994).
- [5] J. M. Pearson, R. C. Nayak, S. Goriely, Phys. Lett. B 387, 455 (1996)
- [6] T. Kautzsch et al., Eur. Phys. J. A 9, 201 (2000).
- [7] I. Dillmann et al., Phys. Rev. Lett. 91, 162503 (2003).
- [8] A. Jungclaus et al., Phys. Rev. Lett. 99, 132501 (2007).
- [9] M. Dworschak et al., Phys. Rev. Lett. 100, 072501 (2008).
- [10] K. L. Jones et al., Nature 465, 454 (2010)
- [11] J. F. Berger, M. Girod, D. Gogny, Nucl. Phys. A 428, 23c (1984)
- [12] R. Rodríguez-Guzmán et al, Nucl. Phys. A709, 201 (2002).
- [13] T.R. Rodríguez and J.L. Egido, Phys. Rev. Lett. 99, 062501 (2007).
- [14] M. Bender et al, Rev. Mod. Phys. 75, 121 (2003).
- [15] M. Anguiano, J. L. Egido, and L. M. Robledo, Nucl. Phys. A696, 467 (2001)

- [16] Evaluated Nuclear Structure Data File, <http://www.nndc.bnl.gov/ensdf/>
- [17] P. Ring and P. Schuck, *The nuclear many body problem*, Springer-Verlag, Berlin, 1980.
- [18] J.L. Egido and L.M. Robledo, in *Extended density functional in nuclear structure physics*, Lect. Notes in Phys. **641**, 269-299 (2004).